Optics Letters

0.85 PW laser operation at 3.3 Hz and high-contrast ultrahigh-intensity $\lambda = 400$ nm second-harmonic beamline

YONG WANG,[1,†,*] SHOUJUN WANG,[1,†] ALEX ROCKWOOD,[2,†] BRADLEY M. LUTHER,[3] REED HOLLINGER,[1] ALDEN CURTIS,[1] CHASE CALVI,[2] CARMEN S. MENONI,[1,3] AND JORGE J. ROCCA[1,2]

[1]Electrical and Computer Engineering Department, Colorado State University, Fort Collins, Colorado 80523, USA
[2]Physics Department, Colorado State University, Fort Collins, Colorado 80523, USA
[3]Chemistry Department, Colorado State University, Fort Collins, Colorado 80523, USA
*Corresponding author: yongw@colostate.edu

Received 26 July 2017; revised 25 August 2017; accepted 28 August 2017; posted 31 August 2017 (Doc. ID 303311); published 22 September 2017

We demonstrate the generation of 0.85 PW, 30 fs laser pulses at a repetition rate of 3.3 Hz with a record average power of 85 W from a Ti:sapphire laser. The system is pumped by high-energy Nd:glass slab amplifiers frequency doubled in LiB_3O_5 (LBO). Ultrahigh-contrast $\lambda = 400$ nm femtosecond pulses were generated in KH_2PO_4 (KDP) with >40% efficiency. An intensity of 6.5×10^{21} W/cm^2 was obtained by frequency doubling 80% of the available Ti:sapphire energy and focusing the doubled light with an $f/2$ parabola. This laser will enable highly relativistic plasma experiments to be conducted at high repetition rate.

OCIS codes: (140.3280) Laser amplifiers; (140.3590) Lasers, titanium; (320.7090) Ultrafast lasers.

https://doi.org/10.1364/OL.42.003828

There is great interest in ultrahigh-intensity laser pulses for relativistic ultrahigh-energy density science, ultrashort-wavelength coherent and incoherent radiation sources, and particle acceleration. The advent of chirped-pulse amplification (CPA) [1] enabled dramatic growth in the peak power of the most powerful lasers [2,3]. Several petawatt (PW) lasers have been demonstrated or are under development in laboratories worldwide [4–11]. New laser systems aimed to generate peak powers of 10 PW also are under development [12–16]. The first laser to achieve the PW power level did so by compressing kJ pulses from an Nd:glass laser to ps pulse duration [4]. Other lasers achieved this peak power level with less energetic pulses of hundreds of J and hundreds of fs pulse duration from Nd:glass amplifiers [5,6]. These lasers typically fire at a repetition rate of several shots per hour. A second class of PW-class lasers produces much less energetic pulses of shorter pulse duration, typically 30 fs or less [7–10]. To date, most PW lasers have been developed with Titanium:Sapphire (Ti:Sa) as the gain medium, which offers broad bandwidth and fs pulse duration [7–17]. Alternatively, the technique of optical parametric CPA applied to PW laser offers the advantages of a wider bandwidth, high temporal contrast, small thermal effects, and tunable wavelength [7,8,10] but with typically lower efficiency. High-power Ti:Sa lasers were demonstrated at the >100 TW peak power level at 10 Hz repetition rate [3]. However, the repetition rate of such lasers decreases greatly as they are scaled to PW, mostly due to heat removal limitations in the pump lasers. The highest peak power achieved to date is a 5.4 PW Ti:Sa laser [9]. The highest repetition rate reported for PW class lasers is 1 Hz [11] and significantly less in most other cases [5,6,8]. A diode-pumped Nd:glass-pumped Ti:Sa laser is under development to generate PW pulses at 10 Hz [18]. Presently in the commissioning phase, this laser has so far been demonstrated to generate 16 J pulses at 3.3 Hz repetition rate that, once compressed, should produce >0.4 PW peak power pulses with an average power >40 W [18]. A Ti:Sa field synthesizer also is under development with the goal of reaching a PW level output at a repetition rate of 10 Hz [19]. While diode pumping of PW lasers has clear advantages for scaling to high repetition rates and increased efficiency, flash lamps still remain greatly more affordable. Here we report the demonstration of a flash-lamp-pumped Ti:Sa laser, which generates 0.85 PW pulses of 30 fs duration at 3.3 Hz repetition rate with a record average power of 85 W after compression. This is the highest average power reported to date for a PW class laser.

The laser setup is schematically illustrated in Fig. 1. It consists of a conventional Ti:Sa front end that delivers $\lambda = 800$ nm pulses into a chain of three high-power Ti:Sa amplification stages pumped by Nd:YAG slab amplifiers designed to operate at repetition rate up to 5 Hz. An 87 MHz Kerr lens mode-locked oscillator (KMLabs) produces 45 nm bandwidth pulses that are stretched to 550 ps FWHM using a grating stretcher [20]. A Pockels cell selects pulses at a frequency of 10 Hz to match the repetition rate of the first two stages of Ti:Sa amplification. These low-energy multipass amplifiers generate 3 mJ and 250 mJ pulses when pumped by a commercially available 600 mJ, 10 Hz, frequency-doubled *Q*-switched Nd:YAG laser (Quanta Ray Pro-270).

The output of this laser front end is further amplified in three multipass Ti:Sa amplifiers pumped by the frequency-doubled output of eight compact flash-lamp-pumped high-energy Nd:glass slab amplifiers, developed at Colorado State University [21]. The front end of the slab laser system consists of a *Q*-switched 1053 nm Nd:YLF oscillator that produces 10 mJ pulses of ~15 ns FWHM duration. The pulses from this oscillator are relay imaged onto a serrated aperture to generate a flat-top beam profile and then spatially filtered to produce a beam with a super-Gaussian intensity profile. This beam profile is relay imaged throughout the rest of the system. The pulses are first amplified to 100 mJ in a flash-lamp-pumped preamplifier consisting of two 7 mm diameter Nd:YLF rods. The beam size is subsequently enlarged and is amplified to 3 J passing through a combination of two 9 mm and two 15 mm Nd:YLF rods, all flash-lamp pumped. The amplified beam is subsequently split into two arms by a 50% beam splitter. Each beam arm is further amplified by an additional 15 mm Nd:YLF amplifier to reach an energy of 3 J. Both circular beams are subsequently stretched onto 8 mm × 120 mm ovals using cylindrical anamorphic imaging telescopes to conform to the 10 mm × 140 mm cross section of the slab amplifiers. The oval beam of each of the two arms is amplified in two passes through the 400 mm length of a Nd:glass slab preamplifier. This preamplifier and the final eight slab amplifiers are similar to those we previously used to pump a 7.5 J, 170 TW, Ti:Sa laser [21]. The narrow slab geometry with zig-zag beam path has long been recognized as a way to eliminate first-order thermal and stress-induced focusing, reduce stress-induced birefringence and increase heat removal to avoid stress induce fracture. This significantly reduces the limitations in the repetition rate inherent to the more commonly used rod geometry [22,23]. Slab amplifiers have been previously used to amplify ns pulses up to 25 J energy [24,25]. Our Nd:glass slab pump laser amplifiers are pumped by four Xe flash lamps, which are driven with 300 μs duration current pulses that deposit ~700 J of electrical energy per lamp per shot. The cooling is provided by turbulent water flow.

Each of the slab preamplifiers is operated to generate 16 J pulses that are divided evenly by three beam splitters (25%, 33%, 50%) to become the input of four identical Nd:glass slab power amplifiers. Amplification of input pulses with 4 J energy in each slab generates pulses with ~18 J energy and 15 ns duration at 1053 nm. The rms pulse energy fluctuation for 1053 nm slab pump laser is ~1%. The amplified beams are reshaped into 22 mm diameter beams that are imaged into 27 mm diameter LBO crystals (CrystalLaser) to generate 11 J pulses at 527 nm. The doubling efficiency is ~63%. A $\lambda/2$ wave plate is placed on each arm before the LBO crystal to ensure *S*-polarization output. The eight slab amplifiers arms produce a total 527 nm pump energy of ~88 J, with a uniform nearly flat-top beam profile.

A 6 J pulse is separated and relay imaged onto the first of three high-power Ti:Sa amplification stages that use a 30 mm diameter, 28 mm thick crystal. Three passes of the 800 nm, 250 mJ seed pulses through this Ti:Sa amplifier produce pulse energies up to 3 J at 3.3 Hz repetition rate. From the remaining laser pump energy, 38 J pulses are relay imaged onto a fourth amplification stage, consisting of a 60 mm diameter, 30 mm

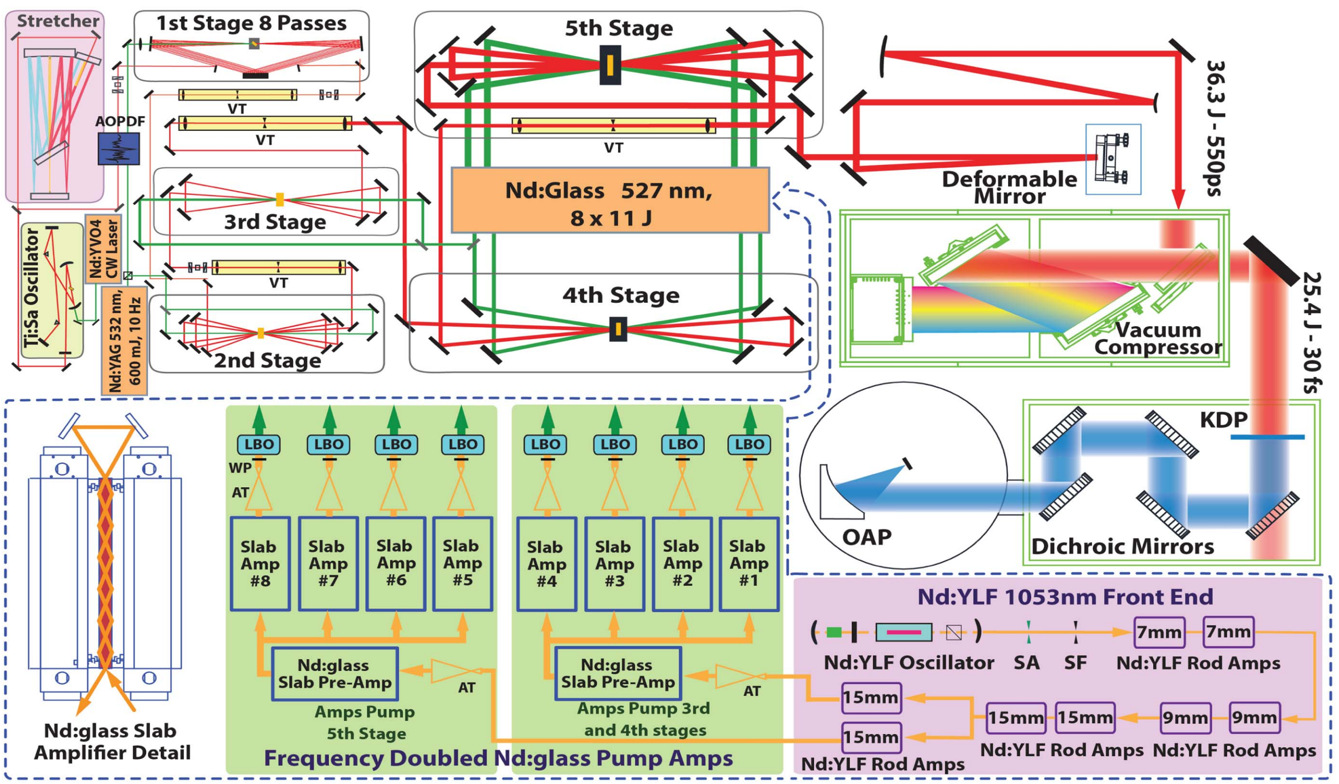

Fig. 1. Diagram of 3.3 Hz, 0.85 PW CPA Ti:Sa laser system. Top: Ti:Sa laser, frequency-doubling setup, and target chamber. Bottom: Pump laser based on Nd:glass slab amplifiers designed to operate at a 5 Hz repetition rate. VT, vacuum tube; SA, serrated aperture; SF, spatial filter; AT, anamorphic telescope; WP, wave plate.

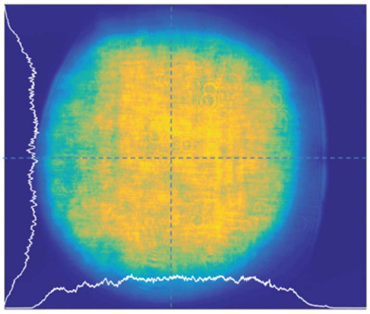

Fig. 2. Spatial single-shot beam profile after the final Ti:Sa booster amplifier operating at full power.

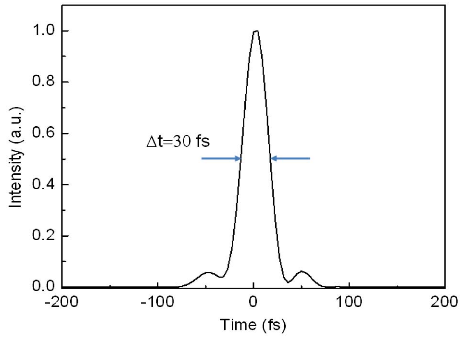

Fig. 4. Autocorrelation trace of the compressed pulses obtained from a single-shot real-time spectral phase measurement.

thick Ti:Sa crystal in which the beam diameter is 45 mm. After two passes, the energy is 13.5 J. The remaining 44 J of laser pump energy are relay imaged onto a fifth stage amplifier, consisting of a 90 mm diameter, 30 mm thick, Ti:Sa crystal (GT Crystal Systems). The output energy can reach >37.6 J after three-pass amplification with a beam size of 55 mm. The crystals of the last two amplification stages are surrounded by flowing methyl salicylate for cooling and suppression of parasitic lasing. Because all the pump beams and the seed beam have flattop spatial profiles, the output beam is close to a homogeneous flattop (Fig. 2).

The evolution of the laser spectrum along the amplifier chain is shown in Fig. 3. An acousto-optic programmable dispersive filter (FASTLITE) is inserted between the stretcher and the first multipass amplifier to compensate for gain narrowing and to control redshift to broaden the bandwidth. The spectral bandwidth after the compressor is 50 nm FWHM. The B integral of the system is estimated to be 1.4.

The output pulses are compressed in a vacuum gratings compressor composed of four 1740 l/mm gold-coated holographic gratings (Lawrence Livermore National Laboratory) [26]. The first and fourth gratings are 42 cm × 21 cm in size, and the second and third gratings are 46 cm × 21 cm in size. The beam diameter is enlarged to 185 mm before entering the compressor using a reflective telescope. The total transmission efficiency of the compressor is 70%, resulting in compressed pulses of up to 26.3 J energy. The temporal intensity profile is reconstructed by a single-shot real-time spectral phase measurement device [27]. The measured compressed pulse duration is 30 fs (Fig. 4), giving a peak power of ∼0.88 PW for the highest energy shots produced. Figure 5 shows the shot-to-shot pulse energy variation measured before compressor for a series of consecutive shots at 3.3 Hz. The average pulse energy is 36.3 J, corresponding to an average power of 120 W before compression. The shot-to-shot energy variation is ∼1.7%rms. The average pulse output energy after compressor is 25.4 J, corresponding to an average peak power of 0.85 PW and to an average power of 85 W. This is the highest average power reported to date from a PW class laser. Operation of the pump laser at its full design goal of 5 Hz could potentially generate an average power of 127 W after compression.

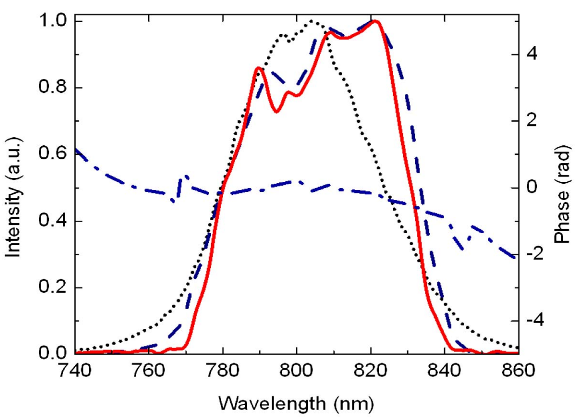

Fig. 3. Evolution of the laser spectra through the system: after stretcher (dotted line); after first power amplifier (dashed line); after compressor (solid line); and the final spectral phase (dash–dotted line).

To enable experiments requiring ultrahigh contrast [28], the 30 fs, $\lambda = 800$ nm laser output pulses were frequency doubled in a 0.8 mm thick antireflection coated KDP crystal. The beam diameter at the crystal is 185 mm. The $\lambda = 400$ nm second harmonic light is separated from the 800 nm fundamental beam using a sequence of five dichroic mirrors with 99.9% reflectivity at $\lambda = 400$ nm and a transmittance of >99.5% at the fundamental wavelength. A first set of frequency-doubling experiments was conducted using up to 80% of the output pulse energy available from the Ti:Sa laser. Figure 6 shows the measured doubling efficiency as a function of the energy impinging on the doubling crystal.

A conversion efficiency >40% is readily obtained for input intensities of 2.5×10^3 GW/cm^2, resulting in $\lambda = 400$ nm pulses of >8 J. Because the contrast of the $\lambda = 800$ nm pulses was measured to be $\sim 5 \times 10^6$, the second-harmonic pulses are inferred to have a contrast $> 1 \times 10^{12}$. Beam focusing is accomplished with an $f/2$ off-axis parabolic mirror (OAP) ($f = 370$ mm). A deformable mirror placed after the last amplifier with Shack Hartmann sensor feedback was used to

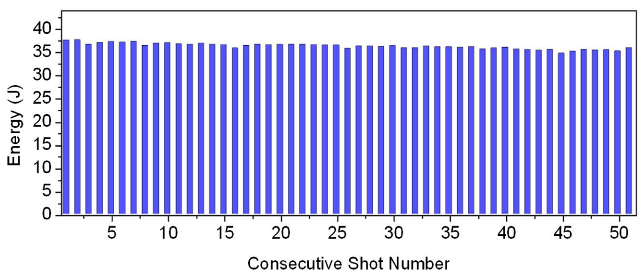

Fig. 5. Shot-to-shot pulse energy variation of Ti:Sa laser pulse before compression at 3.3 Hz repetition rate.

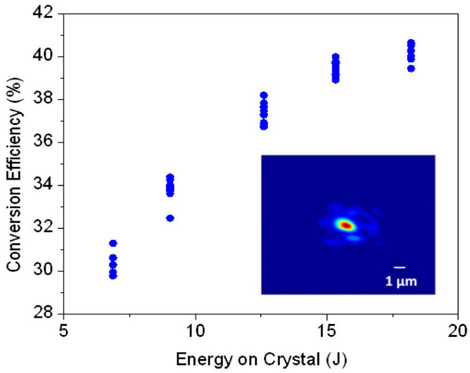

Fig. 6. Doubling efficiency as a function of input pulse energy. Inset: Spot focus with $f/2$ parabolic mirror at $\lambda = 400$ nm.

minimize the spot focus diameter to ~1.2 μm FWHM (Fig. 6 inset), corresponding to an intensity of $\sim 6.5 \times 10^{21}$ W/cm^2. The use of an $f/1$ OAP will allow us to reach intensities $>2 \times 10^{22}$ W/cm^2. An even higher intensity will be obtained using the full energy of the pulses generated by the PW class Ti:Sa laser.

In conclusion, we have demonstrated a Ti:Sa CPA laser that generates 0.85 PW pulses of 30 fs duration at 3.3 Hz repetition rate. This laser is enabled by a frequency-doubled high-energy flash-lamp-pumped Nd:glass zig-zag slab pump laser designed to operate at repetition rates up to 5 Hz with good beam quality. Pulses containing 80% of the maximum available energy were frequency doubled to generate ultrahigh-contrast $\lambda = 400$ nm fs pulses, which were focused to obtain an intensity of 6.5×10^{21} W/cm^2. Intensities $>2 \times 10^{22}$ W/cm^2 will be obtainable using $f/1$ focusing optics. This PW-class laser will enable relativistic plasma experiments at high repetition rate and will extend high repetition rate soft x-ray lasers to shorter wavelengths.

Funding. Air Force Office of Scientific Research (AFOSR) (FA9550-14-1-0232, FA9550-16-1-0286); U.S. Department of Energy (DOE) (DE-SC0014610); NESTec.

Acknowledgment. This material is based upon work supported by the Air Force Office of Scientific Research and the Fusion Science Program of the Office of Science, US Dept. of Energy. Previous support from NSF (MRI-ARRA 09-561) is acknowledged, along with valuable contributions of Mark Woolston, Dale Martz, David Alessi, and Oscar Martinez.

[†]These authors contributed equally to this work.

REFERENCES

1. D. Strickland and G. Mourou, Opt. Commun. **56**, 219 (1985).
2. C. P. J. Barty, T. Guo, C. Le Blanc, F. Raksi, C. Rose-Petruck, J. Squier, K. R. Wilson, V. V. Yakovlev, and K. Yamakawa, Opt. Lett. **21**, 668 (1996).
3. K. Yamakawa, M. Aoyama, S. Matsuoka, T. Kase, Y. Akahane, and H. Takuma, Opt. Lett. **23**, 1468 (1998).
4. M. D. Perry, D. Pennington, B. C. Stuart, G. Tietbohl, J. A. Britten, C. Brown, S. Harman, B. Golick, M. Kartz, J. Miller, H. T. Powell, M. Vergino, and V. Yanovsky, Opt. Lett. **24**, 160 (1999).
5. E. W. Gaul, M. M. Joel Blakeney, A. Jochmann, M. Ringuette, D. Hammond, T. Borger, R. Escamilla, S. Douglas, W. Henderson, G. Dyer, A. Erlandson, R. Cross, J. Caird, C. Ebbers, and T. Ditmire, Appl. Opt. **49**, 1676 (2010).
6. Y. Kitagawa, H. Fujita, R. Kodama, H. Yoshida, S. Matsuo, T. Jitsuno, T. Kawasaki, H. Kitamura, T. Kanabe, S. Sakabe, K. Shigemori, N. Miyanaga, and Y. Izawa, IEEE J. Quantum Electron. **40**, 281 (2004).
7. J. H. Sung, H. W. Lee, J. Y. Yoo, J. W. Yoon, C. W. Lee, J. M. Yang, Y. J. Son, Y. H. Jang, S. K. Lee, and C. H. Nam, Opt. Lett. **42**, 2058 (2017).
8. Z. Wang, C. Liu, Z. Shen, Q. Zhang, H. Teng, and Z. Wei, Opt. Lett. **36**, 3194 (2011).
9. Z. Gan, L. Yu, S. Li, C. Wang, X. Liang, Y. Liu, W. Li, Z. Guo, Z. Fan, X. Yuan, L. Xu, Z. Liu, Y. Xu, J. Lu, H. Lu, D. Yin, Y. Leng, R. Li, and Z. Xu, Opt. Express **25**, 5169 (2017).
10. X. Zeng, K. Zhou, Y. Zuo, Q. Zhu, J. Su, X. Wang, X. Wang, X. Huang, X. Jiang, D. Jiang, Y. Guo, N. Xie, S. Zhou, Z. Wu, J. Mu, H. Peng, and F. Jing, Opt. Lett. **42**, 2014 (2017).
11. K. Nakamura, H.-S. Mao, A. J. Gonsalves, H. Vincenti, D. E. Mittelberger, J. Daniels, A. Magana, C. Toth, and W. P. Leemans, IEEE J. Quantum Electron. **53**, 1 (2017).
12. L. Xu, L. Yu, X. Liang, Y. Chu, Z. Hu, L. Ma, Y. Xu, C. Wang, X. Lu, H. Lu, Y. Yue, Y. Zhao, F. Fan, H. Tu, Y. Leng, R. Li, and Z. Xu, Opt. Lett. **38**, 4837 (2013).
13. G. Mourou, G. Korn, W. Sandner, and J. L. Collier, *ELI—Extreme Light Infrastructure: Science and Technology with Ultra-Intense Lasers Whitebook* (Thoss Media GmbH, 2011).
14. C. Hernandez-Gomez, S. P. Blake, O. Chekhlov, R. J. Clarke, A. M. Dunne, M. Galimberti, S. Hancock, R. Heathcote, P. Holligan, A. Lyachev, P. Matousek, I. O. Musgrave, D. Neely, P. A. Norreys, I. Ross, Y. Tang, T. B. Winstone, B. E. Wyborn, and J. Collier, J. Phys. Conf. Ser. **244**, 032006 (2010).
15. E. Khazanov, *Nonlinear Optics: East-West Reunion* (Institute of Applied Physics, 2011).
16. J. P. Zou, "Design and current progress of the Apollon 10 PW project," presented at the 1st International Symposium on High Power Laser Science and Engineering (HPLSE), Suzhou, China, 2014.
17. S. Backus, C. G. Durfee III, M. M. Murnane, and H. C. Kapteryn, Rev. Sci. Instrum. **69**, 1207 (1998).
18. E. Sistrunk, T. Spinka, A. Bayramian, P. Armstrong, S. Baxamusa, S. Betts, D. Bopp, S. Buck, K. Charron, J. Cupal, R. Demaret, R. Deri, J. Nicola, M. Drouin, A. Erlandson, S. Fulkerson, C. Gates, J. Horner, J. Horacek, J. Jarboe, K. Kasl, D. Kim, E. Koh, L. Koubikova, R. Lanning, J. Lusk, W. Maranville, C. Marshall, D. Mason, P. Mazurek, J. Menapace, P. Miller, J. Naylon, J. Nissen, J. Novak, D. Peceli, P. Rosso, K. Schaffers, T. Silva, D. Smith, J. Stanley, R. Steele, C. Stolz, S. Telford, J. Thoma, D. VanBlarcom, J. Weiss, P. Wegner, B. Rus, and C. Haefner, *Conference on Lasers and Electro-Optics*, OSA Technical Digest (Optical Society of America, 2017), paper STh1L.2.
19. S. Karsch, Z. Major, J. Fülöp, I. Ahmad, T. Wang, A. Henig, S. Kruber, R. Weingartner, M. Siebold, J. Hein, C. Wandt, S. Klingebiel, J. Osterhoff, R. Hörlein, and F. Krausz, *Advanced Solid-State Photonics*, OSA Technical Digest Series (Optical Society of America, 2008), paper WF1.
20. O. E. Martínez, J. P. Gordon, and R. L. Fork, J. Opt. Soc. Am. A **1**, 1003 (1984).
21. D. H. Martz, D. Alessi, B. M. Luther, Y. Wang, D. Kemp, M. Berrill, and J. J. Rocca, Opt. Lett. **35**, 1632 (2010).
22. W. S. Martin and J. P. Chernoch, "Multiple internal reflection face-pumped laser," U.S. patent 3,633,126 (January 4, 1972).
23. J. Eggleston, T. Kane, K. Kuhn, J. Unternahrer, and R. Byer, IEEE J. Quantum Electron. **20**, 289 (1984).
24. C. B. Dane, L. E. Zapata, W. A. Neuman, M. A. Norton, and L. A. Hackel, IEEE J. Quantum Electron. **31**, 148 (1995).
25. M. J. Shoup, J. H. Kelly, and D. L. Smith, Appl. Opt. **36**, 5827 (1997).
26. J. A. Britten, M. D. Perry, B. W. Shore, and R. D. Boyd, Opt. Lett. **21**, 540 (1996).
27. T. Oksenhendler, S. Courdreau, N. Forget, V. Crozatier, S. Grabielle, R. Herzog, O. Gobert, and D. Kaplan, Appl. Phys. B **99**, 7 (2010).
28. C. Bargsten, R. Hollinger, M. Gabriela Capeluto, V. Kaymak, A. Pukhov, S. Wang, A. Rockwood, Y. Wang, D. Keiss, R. Tommasini, R. London, J. Park, M. Busquet, M. Klapisch, V. N. Shlyaptsev, and J. J. Rocca, Sci. Adv. **3**, e1601558 (2017).